Mixed Transition Metal-Main Group Atom Clusters as Potential Models for M_2X (010) and M_4 (100) Surfaces. Synthesis and Spectroscopic and Structural Characterization of $M_4(CO)_{13}(\mu_3\text{-PPh})$ (M = Ru, Os). Pyramidal Clusters with M_3P Square Faces

Andrew A. Cherkas, John F. Corrigan, Simon Doherty, Shane A. MacLaughlin, Françoise van Gastel, Nicholas J. Taylor, and Arthur J. Carty*

Guelph-Waterloo Centre for Graduate Work in Chemistry, Waterloo Campus, Department of Chemistry, University of Waterloo, Waterloo, Ontario, Canada N2L 3G1

Received October 9, 1992

The clusters $HM_3(CO)_{10}(\mu\text{-PPh}_2)$ (M = Ru (**1a**), Os (**1b**)) are shown to be convenient precursors of the phosphinidene-stabilized clusters *nido*-$M_4(CO)_{13}(\mu_3\text{-PPh})$ (M = Ru (**2a**), Os (**2b**)) via P-C(Ph) activation, reductive elimination of benzene, and condensation. Heating a toluene solution of **1a** under a purge of carbon monoxide forms $Ru_4(CO)_{13}(\mu_3\text{-PPh})$ (40%) as the major product. Formation of $Os_4(CO)_{13}(\mu_3\text{-PPh})$ requires more forcing conditions. Heating a solid sample of **1b** at 215 °C for 8 min affords **2b** in 20-25% yield. Both **2a** and **2b** have been characterized by spectroscopy and by accurate single-crystal X-ray structure analyses. Crystals of **2a** and **2b** are isomorphous, crystallizing in the orthorhombic space group $P2_12_12_1$ with the following unit cell dimensions: **2a**, a = 11.031(2), b = 12.366(2), and c = 18.094 Å, with Z = 4; **2b**, a = 11.055(3), b = 12.344(3), and c = 18.016(5) Å, with Z = 4. The molecular structures of **2a** and **2b** possess M_4P cluster frameworks containing a butterfly arrangement of metal atoms stabilized by a μ_3-phosphinidene fragment capping an open triangular face. Both clusters adhere to the effective atomic number rule (62 electrons) and are associated with nido octahedral M_4P core geometries when the skeletal bonding electrons are considered (seven skeletal electron pairs, five vertices). In the latter instance the "PPh" fragment is located in the square basal plane of the pyramidal framework. An alternative, less time-consuming procedure for the preparation of $Ru_4(CO)_{13}(\mu_3\text{-PPh})$ (**2a**) is also described. Dropwise addition of dichlorophenylphosphine to a concentrated THF solution of the dianion $K_2[Ru_4(CO)_{13}]$ affords **2a** in reasonable yields. Variable-temperature ^{13}C NMR studies of **2a** revealed four independent dynamic processes involving localized CO exchange, and a direct comparison is drawn between **2a** and $(\mu\text{-H})_2Ru_4(CO)_{12}(\mu_3\text{-PPh})$. At temperatures in excess of 296 K, we have observed the onset of total intermetallic CO scrambling. The potential of clusters **2a** and **2b** to serve as molecular models for catalytically active transition metal and transition metal-main group surfaces as well as potential precursors to square planar metal clusters stabilized by μ_4-phosphinidene ligands are discussed.

Introduction

The activation of small molecules at a polymetallic center and the modeling of molecular interactions at metal and metal-nonmetal surfaces are major incentives for the continued development of metal-cluster chemistry.[1] Recent studies in the latter area include the characterization of benzyne-coordinated tetra- and pentaruthenium clusters as molecular models for the dissociative chemisorption of benzene at a stepped catalytically active site on a metal (111) surface,[2] while the nondissociative chemisorption of benzene at a 3-fold site on the surface of a close-packed lattice has been mimicked by the cluster $[Os_3(CO)_9(\mu_3\text{-}\eta^2\text{:}\eta^2\text{:}\eta^2\text{-}C_6H_6)]$.[3] The development of such models remains fundamental to our understanding of surface chemistry at the molecular level, and since the formulation of the cluster-surface analogy by Muetterties[4] and others,[5] this approach has been utilized extensively.[6] In principle, there exists an extensive array of clusters of differing nuclearities available for surface modeling studies ranging from the metal-metal-bonded dimer[7] to clusters with ten or more metal atoms often structurally comparable to a fragment of the bulk metallic lattice.[8] However, for reasons of simplicity and ready availability, by far the most widely used cluster types are those containing three mutually bonded metal atoms which mimic a 3-fold site in a close packed array of metal atoms.[1,3] The dominant obstacle to the use of high-nuclearity clusters remains their inaccessibility (in workable quantities) by conventional synthetic routes.[9]

The butterfly cluster arrangement of metal atoms has attracted

(1) (a) Humphries, A. P.; Kaesz, H. D. *Prog. Inorg. Chem.* **1979**, *25*, 145. (b) Davies, S. C.; Kablunde, K. J. *Chem. Rev.* **1982**, *82*, 153. (c) Arif, A. M.; Bright, T. A.; Jones, R. A.; Nunn, C. M. *J. Am. Chem. Soc.* **1988**, *110*, 5389. (d) Adams, R. D.; Horvath, I. T. *Prog. Inorg. Chem.* **1986**, *73*, 126. (e) Raithby, P. R.; Rosales, M. J. *Adv. Inorg. Chem. Radiochem.* **1985**, *29*, 169. (f) Sappa, E.; Tiripicchio, A.; Braunstein, P. *Chem. Rev.* **1983**, *83*, 203. (g) Amoroso, A. J.; Gade, L. H.; Johnson, B. F. G.; Lewis, J.; Raithby, P. R.; Wong, W. T. *Angew. Chem., Int. Ed. Engl.* **1991**, *30*, 107.

(2) (a) Knox, S. A. R.; Lloyd, B. R.; Orpen, A. G.; Vinas, J. M.; Weber, M. *J. Chem. Soc., Chem. Commun.* **1987**, 1498. (b) Knox, S. A. R.; Lloyd, B. R.; Morton, D. A. V.; Nicholls, S. M.; Orpen, A. G.; Vinas, J. M.; Weber, M.; Williams, G. K. *J. Organomet. Chem.* **1990**, *394*, 385.

(3) (a) Johnson, B. F. G.; Lewis, J.; Gallup, M.; Martinelli, M. *Discuss. Faraday Soc.* **1991**, *92*, 241. (b) Gallop, M. A.; Gomez-Sal, M. P.; Housecroft, C. E.; Johnson, B. F. G.; Lewis, J.; Owen, S. M.; Raithby, P. R.; Wright, A. H. *J. Am. Chem. Soc.* **1992**, *114*, 2502.

(4) (a) Muetterties, E. L. *Angew. Chem., Int. Ed. Engl.* **1978**, *17*, 545. (b) Muetterties, E. L.; Rhodin, T. N.; Band, E.; Brucker, C. F.; Pretzer, W. *Chem. Rev.* **1979**, *79*, 91. (c) Muetterties, E. L. *Pure Appl. Chem.* **1982**, *54*, 83. (d) Muetterties, E. L. *Chem. Soc. Rev.* **1982**, 283. (e) Muetterties, E. L.; Krause, M. J. *Angew. Chem., Int. Ed. Engl.* **1983**, *22*, 135.

(5) (a) Evans, J. *Chem. Soc. Rev.* **1981**, *10*, 159. (b) Somorjai, G. A. *Chem. Soc. Rev.* **1983**, 321. (c) Ertl, G. In *Metal Clusters in Catalysis*; Gates, B. C., Guczi, J., Knozinger, H., Eds.; Elsevier: Amsterdam, 1986. (d) Braunstein, P. *Nouv. J. Chim.* **1986**, *10*, 365. (e) Wadepohl, H. *Angew Chem., Int. Ed. Engl.* **1992**, *31*, 247.

(6) Weigand, B. C.; Freind, C. M. *Chem. Rev.* **1992**, *92*, 491.

(7) Riera, V.; Ruiz, M. A.; Villafane, F. *Organometallics* **1992**, *11*, 2854. (b) Chini, P. *J. Organomet. Chem.* **1980**, *29*, 1. (c) Muetterties, E. L.; Stein, J. *Chem. Rev.* **1979**, *79*, 479.

(8) (a) Albano, V. G.; Ceriotti, A.; Chini, P.; Ciani, G.; Martinengo, S.; Naker, M. *J. Chem. Soc., Chem. Commun.*, **1975**, 859. (b) Jackson, P. F.; Johnson, B. F. G.; Lewis, J.; Nelson, W. J. H.; McPartlin, M. *J. Chem. Soc., Dalton Trans.* **1982**, 2099. (c) Ciani, G.; Sironi, A.; Martinengo, S. *J. Chem. Soc., Dalton Trans.* **1982**, 1099. (d) Martinengo, S.; Ciani, G.; Sironi, A. *J. Am. Chem. Soc.* **1980**, *102*, 7565. (e) Chini, P. *J. Organomet. Chem.* **1980**, *200*, 37.

(9) Bantel, H.; Hansert, B.; Powell, A. K.; Vahrenkamp, H. *Angew. Chem., Int. Ed. Engl.* **1989**, *28*, 1059.

0020-1669/93/1332-1662$04.00/0

considerable attention,[10] a consequence of both its structural and electronic versatility.[11] We[12] and others[4b,13] have recognized the potential of these M_4 frameworks (dihedral angles 90–180°) to serve as models for the chemisorption of small unsaturated molecules and for C–X bond forming/cleavage reactions occurring at a stepped catalytically active site on a metal surface. In addition to the close resemblance of the geometrical arrangement of metal atoms in *nido*-$Ru_4(CO)_{13}(\mu_3\text{-PPh})$ to a stepped metal surface, its main group–metal atom framework (M_3P square face) bears a remarkably close similarity to the atomic connectivity of ruthenium and phosphorus in ruthenium phosphide, Ru_2P (010).[14]

The chemistry of M_4 clusters and their applications as models remain less well developed than those for their M_3 counterparts in part due to the lack of rational synthetic procedures coupled with facile fragmentation pathways often observed for unsupported metal atom frameworks. Herein we report the synthesis and spectroscopic and structural characterization of two phosphinidene-stabilized clusters $M_4(CO)_{13}(\mu_3\text{-PPh})$ (M = Ru (**2a**), Os (**2b**)) as potential models for metal and metal–main group atom surfaces. Clusters **2a** and **2b** have proven to be remarkably stable to fragmentation under a variety of conditions.[12,15] We also note that the skeletal rearrangement of the M_4-butterfly skeleton to a square M_4 array offers an extension to further models (ruthenium (100)).

Experimental Section

General Procedures. Standard double-manifold vacuum-line techniques were used for chemical manipulations, and all reactions were performed under an atmosphere of dry dinitrogen unless otherwise stated. All solvents were dried prior to use, hexane and tetrahydrofuran over sodium/benzophenone, dichloromethane and acetonitrile over P_2O_5, and xylenes and toluene over $LiAlH_4$.

Reactions were monitored by IR spectroscopy and thin-layer chromatography (Baker Flex, silica gel, 1B-F). Product purification was performed either by column chromatography (330 × 30 mm) with silica gel (70–230 mesh) or by thin-layer chromatography on silica gel plates (20 × 20 cm, Merck, TLC grade, Aldrich Chemical Co.). Solution infrared spectra were recorded on a Nicolet-520 FTIR spectrometer using sodium chloride cells. NMR spectra were recorded on Bruker AM-250 and AC-200 instruments, and chemical shifts were referenced internally to the solvents CD_2Cl_2 and $CDCl_3$ (^1H and $^{13}C\{^1H\}$) and externally to 85% H_3PO_4 ($^{31}P\{^1H\}$). Microanalyses were performed by Guelph Chemical Laboratories Guelph, Ontario.

All chemicals were obtained from commercial sources and used without further purification with the exceptiom of trimethylamine oxide, which was freshly sublimed under vacuum (60 °C, 0.05 Torr, 16 h) prior to use.[16a]

The clusters $(\mu\text{-H})Ru_3(CO)_{10}(\mu\text{-PPh}_2)$ (**1a**),[17] $(\mu\text{-H})Os_3(CO)_{10}(\mu\text{-PPh}_2)$ (**1b**),[16] and $K_2[Ru_4(CO)_{13}]$[18] were prepared by standard literature procedures.

Preparation of $Ru_4(CO)_{13}(\mu_3\text{-PPh})$ (2a). Heating a solution of **1a** (3.54 g, 4.6 mmol) in toluene (150 mL) at reflux purged with a steady stream of CO gas resulted in the formation of a deep purple homogeneous solution. Thin-layer chromatography and IR analysis were used to maximize the formation of **2a**. Reflux was maintained for 150 min. The resulting solution was cooled to room temperature and the solvent removed in vacuo to leave an oily residue. This residue was dissolved in the minimum volume of dichloromethane (10–12 mL); the solution was absorbed onto silica gel, desolvated, placed on a 330 × 30 mm silica gel column and eluted with hexane to afford seven well-separated bands. The first yellow band to elute was identified as $Ru_3(CO)_{12}$, the second red/purple band as $Ru_4(CO)_{13}(\mu_3\text{-PPh})$ (1.04 g, 1.2 mmol, 34%), and the third green fraction as $Ru_5(CO)_{15}(\mu_4\text{-PPh})$.[19] The next fraction contained a mixture of yellow $(\mu\text{-H})_2Ru_3(CO)_8(\mu\text{-PPh}_2)_2$[20] and $Ru_2(CO)_6(\mu\text{-PPh}_2)_2$[21] followed by $(\mu_3\text{-H})Ru_5(CO)_{13}(\mu_4\text{-PPh})(\mu\text{-PPh}_2)$.[22] The remaining two fractions, deep green followed by dark brown, have previously been characterized as $Ru_7(CO)_{18}(\mu_4\text{-PPh})_2$[23] and $Ru_8(CO)_{21}(\mu_6\text{-P})(\mu_4\text{-PPh})(\mu\text{-PPh}_2)$,[24] respectively. The identity of these slower moving fractions was established by comparing their spectroscopic properties with those previously reported. Crystals of **2a** were obtained by cooling a dichloromethane/benzene mixture at –20 °C overnight.

Anal. Calcd for $C_{19}H_5O_{13}PRu_4$: C, 26.03; H, 0.57. Found: C, 25.99; H, 0.70. IR (ν(CO), cm^{-1}, C_6H_{12}): 2097 (w), 2062 (vs), 2050 (s), 2042 (s), 2022 (w), 2012 (m), 1990 (w), 1969 (w, sh). $^{31}P\{^1H\}$ NMR (101.3 MHz, $CDCl_3$, δ): 409.0 (s). $^{13}C\{^1H\}$ NMR (62.0 MHz, CD_2Cl_2, 196 K, δ): 205.2 (d, CO, $^2J_{PC}$ = 70.4 Hz), 200.7 (d, CO, $^2J_{PC}$ = 13.3 Hz), 197.8 (d, CO, $^2J_{PC}$ = 5.0 Hz), 195.8 (s, CO), 191.7 (s, CO), 191.1 (d, CO, $^2J_{PC}$ = 4.4 Hz), 187.8 (d, CO, $^2J_{PC}$ = 9.5 Hz), 184.9 (d, CO, $^2J_{PC}$ = 5.0 Hz), 150.9 (d, C ipso, $^1J_{PC}$ = 12.9 Hz), 130.4 (d, C ortho, $^2J_{PC}$ = 11.1 Hz), 130.4 (s, C para), 128.0 (d, C meta, $^3J_{PC}$ = 9.6 Hz). ^1H NMR (250.0 MHz, $CDCl_3$, δ): 8.0 (m, C_6H_5, 2H), 7.2 (m, C_6H_5, 3H).

Preparation of $Os_4(CO)_{13}(\mu_3\text{-PPh})$ (2b). An evacuated Schlenk tube containing solid $(\mu\text{-H})Os_3(CO)_{10}(\mu\text{-PPh}_2)$ (**1b**) (0.158 g, 0.15 mmol) was heated in an oven at 215 °C for 8 min, during which the orange crystalline material melted to leave a dark brown solid residue upon cooling to room temperature. Extraction into dichloromethane followed by thin-layer chromatography (eluant: dichloromethane/hexane, 20:80 v/v) afforded two major products. The first band to elute was initially identified as deep red $Os_4(CO)_{13}(\mu_3\text{-PPh})$, subsequently confirmed by single-crystal X-ray analysis. Crystals of **2b** were obtained from a dichloromethane/hexane solution at –20 °C (0.025 g, 21%). A deep yellow/orange band following **2b** was identified as $(\mu\text{-H})_2Os_3(CO)_9\{P(Ph)C_6H_4\}$ by comparison of its spectroscopic properties with those previously described.[25]

Anal. Calcd for $C_{19}H_5O_{13}Os_4P$: C, 18.51; H, 0.41. Found: C, 18.21; H, 0.38. IR (ν(CO), cm^{-1}, C_6H_{12}): 2100 (m), 2066 (m, sh), 2060 (vs), 2053 (s), 2043 (s), 2033 (w), 2022 (w), 2014 (w), 2005 (s), 1992 (w), 1978 (w). $^{31}P\{^1H\}$ NMR (101.3 MHz, $CDCl_3$, δ): 191.1 (s). $^{13}C\{^1H\}$ NMR (50.3 MHz, $CDCl_3$, 298 K, δ): 178.7 (d, CO, $^2J_{PC}$ = 5.0 Hz), 172.3 (s, CO), 162.1 (d, CO, $^2J_{PC}$ = 16.0 Hz), 140.0 (d, C ipso, $^1J_{PC}$ =

(10) (a) Sappa, E.; Tiripicchio, A.; Carty, A. J.; Toogood, G. E. *Prog. Inorg. Chem.* **1987**, *35*, 437. (b) Steinmetz, G. R.; Harley, D. A.; Geoffroy, G. L. *Inorg. Chem.* **1980**, *19*, 2985. (c) Braga, D.; Johnson, B. F. G.; Lewis, J.; Mace, J. M.; McPartlin, M.; Puga, J.; Nelson, W. J. H.; Raithby, P. R.; Whitmire, K. H. *J. Chem. Soc., Chem. Commun.* **1982**, 1082.

(11) (a) Carty, A. J.; MacLaughlin, S. A.; Van Wagner, J.; Taylor, N. J. *Organometallics* **1982**, *1*, 1013. (b) Churchill, M. R.; Bueno, C.; Young, D. A. *J. Organomet. Chem.* **1981**, 139. (c) Hogarth, G.; Phillips, J. A.; van Gastel, F.; Taylor, N. J.; Marder, T. B.; Carty, A. J. *J. Chem. Soc., Chem. Commun.* **1988**, 1570. (d) Harris, S.; Blohm, M. L.; Gladfelter, W. L. *Inorg. Chem.* **1989**, *28*, 2290.

(12) Corrigan, J. F.; Doherty, S.; Taylor, N. J.; Carty, A. J. *Organometallics*, in press.

(13) (a) Osella, D.; Ravera, M.; Nervi, C.; Housecroft, C. E.; Raithby, P. R.; Zanelo, P.; Laschi, F. *Organometallics* **1991**, *10*, 3253. (b) Rossi, S.; Pursiainen, J.; Pakkanen, T. A. *Organometallics* **1991**, *10*, 1390. (c) Rumin, R.; Robin, F.; Petillon, F. Y.; Muir, K. W.; Stevenson, I. *Organometallics* **1991**, *10*, 2274.

(14) (a) Rundqvist, S. *Acta Chem. Scand.* **1960**, *14*, 1961. (b) Corbridge, D. E. C. In *The Structural Chemistry of Phosphorus*; Elsevier Scientific Publishing Co.: Amsterdam, 1974, Chapter 3.

(15) Corrigan, J. F.; Doherty, S.; Taylor, N. J.; Carty, A. J. *J. Chem. Soc., Chem. Commun.* **1991**, 1640.

(16) (a) Nicholls, J. N.; Vargas, M. D. *Inorg. Synth.* **1989**, *26*, 289. (b) Colbran, S. B.; Johnson, B. F. G.; Lewis, J.; Sorrell, R. M. *J. Organomet. Chem.* **1985**, *296*, C1.

(17) Nucciarone, D.; MacLaughlin, S. A.; Carty, A. J. *Inorg. Synth.* **1989**, *26*, 264.

(18) Bhattacharyya, A. A.; Nagel, C. C.; Shore, S. G. *Organometallics* **1983**, *2*, 1187.

(19) Natarajan, K.; Zsolnai, L.; Huttner, G. *J. Organomet. Chem.* **1981**, *209*, 85.

(20) Patel, V. D.; Cherkas, A. A.; Nucciarone, D.; Taylor, N. J.; Carty, A. J. *Organometallics* **1986**, *5*, 1498.

(21) (a) Bruce, M. I.; Shaw, G.; Stone, F. G. A. *J. Chem. Soc., Dalton Trans.* **1972**, 2094. (b) Rosen, R. D.; Geoffroy, G. L.; Bueno, C.; Churchill, M. R.; Ortega, R. B. *J. Organomet. Chem.* **1983**, *254*, 89. (c) Patel, V. D.; Cherkas, A. A.; Nucciarone, D.; Taylor, N. J.; Carty, A. J. *Organometallics*, **1985**, *4*, 1792. (d) Bullock, L. M.; Field, J. S.; Haines, R. J.; Minshall, E.; Moore, M. H.; Mulla, F.; Smit, D. N.; Steer, L. M. *J. Organomet. Chem.* **1990**, *381*, 429. (e) Field, J. S.; Haines, R. J.; Mulla, F. *J. Organomet. Chem.* **1990**, *389*, 227. (f) He, Z.; Jugan, N.; Neibecker, D.; Mathieu, R.; Bonnet, J. J. *J. Organomet. Chem.* **1992**, *426*, 247. (g) Beguin, A.; Bottcher, H.-C.; Süss-Fink, G.; Walther, B. *J. Chem. Soc., Dalton Trans.* **1992**, 2133.

(22) Kwek, K. L. M. Ph.D. Thesis, University of Waterloo, 1989.

(23) van Gastel, F.; Taylor, N. J.; Carty, A. J. *J. Chem. Soc., Chem. Commun.* **1987**, 1049.

(24) van Gastel, F.; Taylor, N. J.; Carty, A. J. *Inorg. Chem.* **1989**, *28*, 384.

(25) Colbran, S. R.; Irele, P. T.; Johnson, B. F. G.; Lahoz, F. J.; Lewis, J.; Raithby, P. R. *J. Chem. Soc., Dalton Trans.* **1989**, 2023.

Table I. Crystal and Intensity Data for $M_4(CO)_{13}(\mu_3\text{-PPh})$ (M = Ru (**2a**), Os (**2b**))

	2a	**2b**
formula	$C_{19}H_5O_{13}PRu_4$	$C_{19}H_5O_{13}POs_4$
fw	876.5	1233.0
space group	$P2_12_12_1$	$P2_12_12_1$
a (Å)	11.031(2)	11.055(3)
b (Å)	12.366(2)	12.344(3)
c (Å)	18.094(2)	18.076(5)
V (Å^3)	2468.0(5)	2466.7(11)
Z	4	4
d_{cal} (g cm^{-3})	2.359	3.320
radiation (Å)	0.710 73	0.710 73
temp (K)	150	150
μ(Mo Kα), cm^{-1}	25.31	206.69
transm factors	0.5110–0.6423	0.0268–0.1159
R,[a] %	1.54	2.66
R_w,[b] %	1.77	2.53

[a] $R = \sum(|F_o| - |F_c|)/\sum F_o$. [b] $R_w = [\sum w(|F_o| - |F_c|)^2/\sum wF_o^2]^{1/2}$.

2.4 Hz), 131.1 (d, C ortho, $^2J_{PC}$ = 13.0 Hz), 131.0 (d, C para, $^4J_{PC}$ = 2.8 Hz), 128.4 (d, C meta, $^3J_{PC}$ = 10.2 Hz). ^{1}H NMR (250 MHz, $CDCl_3$, δ): 7.50–7.24 (m, C_6H_5).

Preparation of $Ru_4(CO)_{13}(\mu_3\text{-PPh})$ from $K_2[Ru_4(CO)_{13}]$. All manipulations were carried out in an inert-atmosphere glovebox.

To a mixture of dodecacarbonyltriruthenium (1.447 g, 2.26 mmol), benzophenone (0.616 g, 3.40 mmol), and potassium (0.133 g, 3.40 mmol) was added THF (20 mL) dropwise over a 2-h period. The solution was stirred vigorously for 24 h, yielding a deep red homogeneous solution of $K_2[Ru_4(CO)_{13}]$. Dichlorophenylphosphine (1.7 mmol, 0.231 mL) was added and the reaction mixture stirred for a further 3 h. The solvent was then removed under reduced pressure, the resultant deep red oily residue extracted into dichloromethane (7–8 mL), and the solution absorbed onto silica gel. After removal of excess solvent, the sample was placed on a 200 × 25 mm silica gel column and eluted with hexane to afford three well-separated bands. The first to elute was identified as dodecacarbonyltriruthenium followed by the major purple fraction containing $Ru_4(CO)_{13}(\mu_3\text{-PPh})$ (0.220 g, 15%). The final band to be identified corresponded to $Ru_5(CO)_{15}(\mu_4\text{-PPh})$,[19] identified by its familiar spectroscopic properties.

X-ray Structure Analyses of 2a and 2b. Dark red crystals of **2a** were grown from a dichloromethane/benzene solution at −20 °C, and those of **2b**, from dichloromethane/hexane. A suitable crystal was chosen, glued to a glass fiber using epoxy resin, and mounted on a goniometer head. Unit cell parameters for each crystal were obtained from least squares refinement of the setting angles of 25 reflections well dispersed in reciprocal space.

Collection and Reduction of Intensity Data. Details of the intensity data collection are given in Table I. The intensity data for both **2a** and **2b** were collected at 150 K on a LT2 equipped Siemens R3m/V diffractometer using graphite-monochromated Mo Kα (λ = 0.710 73 Å) radiation and the ω scan technique with a variable scan speed to optimize weak reflections. Background measurements were made at the beginning and end of each scan, each for 25% of the total scan time. Two standard reflections monitored every 100 measurements showed no significant deviations during the data collection. Reflections were flagged as unobserved when $F < 6.0\sigma(F)$ where σ was derived from counting statistics.

Solution and Refinement of the Intensity Data. Patterson syntheses readily yielded the positions of all the metal atoms in both cases, and standard Fourier methods were used to locate the remaining non-hydrogen atoms in the molecule. Full-matrix least-squares refinement of positional and thermal parameters, subsequent conversion to anisotropic coefficients for all non-hydrogen atoms, and several further cycles of least-squares refinement followed. At this stage, for each structure a difference Fourier map revealed the positions of all the hydrogen atoms. In subsequent refinements to convergence, the hydrogen atoms of **2a** were included in calculated positions with refined isotropic thermal parameters whereas those of **2b** were also included in calculated positions with fixed isotropic thermal parameters. The function minimized in the least-squares calculations was $\sum w(|F_o| - |F_c|)^2$. The weighted R value is defined as $R_w = [\sum w(|F_o| - |F_c|)^2/\sum w|F_o|]^{1/2}$ where the weights w optimize on moderate intensities [$w^{-1} = \sigma^2(F)$]. Absorption corrections for **2a** and **2b** were applied by the face-indexed numerical procedure. The atomic scattering factors used including anomalous dispersion corrections were taken from ref 26; for hydrogen, those of Stewart et al. were used.[27] All calculations were performed on a Microvax II using SHELXTL PLUS software. The final R and R_w values are given in Table I (**2a**, 5316 observed reflections, 340 parameters refined; **2b**, 3377 observed reflections, 335 parameters refined). The final difference Fourier maps exhibited minimum and maximum residuals of 0.41 and −0.39 e Å^{-3} and 2.01 and −1.54 e Å^{-3}, for **2a** and **2b**, respectively, in the vicinity of the metal atoms.

Compounds **2a** and **2b** crystallize as isomorphs, in the noncentrosymmetric space group $P2_12_12_1$. Friedel opposites in the ranges $-15 \le h \le 15$, $-17 \le k \le 17$, and $-25 \le l \le 25$ for **2a** and $-17 \le h \le 17$, $-19 \le k \le 19$, and $-28 \le l \le 28$ for **2b** were collected. In both instances, we found the correct enantiomorph (absolute structure) to be indeterminant from the merged data. However, using the unmerged Friedel pairs (**2a**, 9563; **2b**, 5848 observed reflections), the models presented here gave R, R_w values of 1.72, 1.97 and 3.04, 2.86 for **2a** and **2b**, respectively. The alternative enantiomorphs gave R, R_w vaules of 1.97, 2.27 and 3.80, 3.83 for **2a** and **2b**, respectively, unequivocally establishing the enantiomorphic nature of the crystal.

Atomic and positional parameters (Tables II and III) and an appropriate selection of bond lengths and angles (Table IV) are listed for **2a** and **2b**, respectively.

Table II. Atomic Coordinates (×10^4) and Equivalent Isotropic Displacement Coefficients (Å^2 × 10^4) for $Ru_4(CO)_{13}(\mu_3\text{-PPh})$ (**2a**)

	x	y	z	U(eq)[a]
Ru(1)	2698.0(2)	5766.6(1)	4594.0(1)	154.9(4)
Ru(2)	3841.1(2)	3756.5(1)	4505.7(1)	134.7(4)
Ru(3)	3976.6(2)	5218.2(1)	3226.0(1)	148.1(4)
Ru(4)	6054.8(2)	4728.6(1)	4105.5(1)	131.9(4)
P(1)	4673.9(5)	5409.5(5)	4938.0(3)	137(1)
O(1)	2600(2)	8225(2)	4582(1)	378(7)
O(2)	136(2)	5306(2)	3972(1)	409(7)
O(3)	1793(2)	5618(2)	6171(1)	342(7)
O(4)	1287(2)	2930(2)	4137(1)	352(6)
O(5)	5392(2)	1760(2)	4154(1)	295(6)
O(6)	3607(2)	2891(2)	6057(1)	311(6)
O(7)	3444(3)	2898(2)	2719(1)	361(7)
O(8)	4751(2)	7568(2)	3574(1)	283(5)
O(9)	1648(2)	5972(2)	2453(1)	374(7)
O(10)	5764(2)	5294(2)	1928(1)	362(6)
O(11)	6738(2)	3090(2)	2882(1)	278(5)
O(12)	7539(2)	6624(2)	3561(1)	312(6)
O(13)	8078(2)	4212(2)	5196(1)	313(6)
C(1)	2603(3)	7306(2)	4571(2)	245(6)
C(2)	1093(3)	5459(2)	4178(1)	259(6)
C(3)	2119(2)	5692(2)	5575(1)	221(6)
C(4)	2228(3)	3264(2)	4274(1)	226(6)
C(5)	4847(2)	2525(2)	4249(1)	200(6)
C(6)	3699(2)	3231(2)	5476(1)	205(6)
C(7)	3623(3)	3717(2)	2983(1)	234(6)
C(8)	4436(2)	6698(2)	3501(1)	206(6)
C(9)	2488(2)	5691(2)	2752(1)	230(6)
C(10)	5108(2)	5256(2)	2404(1)	224(6)
C(11)	6511(2)	3688(2)	3334(1)	193(6)
C(12)	6979(2)	5908(2)	3760(1)	195(6)
C(13)	7299(2)	4391(2)	4798(1)	191(5)
C(14)	5063(2)	5631(2)	5906(1)	173(5)
C(15)	5716(2)	4890(2)	6323(1)	222(6)
C(16)	5978(3)	5105(3)	7063(1)	297(8)
C(17)	5599(3)	6063(3)	7382(2)	350(9)
C(18)	4973(3)	6810(3)	6974(2)	327(8)
C(19)	4700(3)	6601(2)	6234(2)	259(7)

[a] Equivalent isotropic U defined as one-third of the trace of the orthogonalized U_{ij} tensor.

Results and Discussions

The major impediment in developing the chemistry of M_4 and higher nuclearity clusters and to understanding their associated properties is the absence of rational preparative methodologies for their synthesis. The problem is further accentuated in many instances by facile cluster fragmentation, which imposes severe

(26) *International Tables for X-ray Crystallography*; Kynoch Press: Birmingham, England, 1974, Vol. 4.
(27) Stewart, R. F.; Davidson, E. R.; Simpson, W. T. *J. Chem. Phys.* **1965**, *42*, 3175.

Table III. Atomic Coordinates (×10⁴) and Equivalent Isotropic Displacement Coefficients (Å² × 10³) for $Os_4(CO)_{13}(\mu_3\text{-PPh})$ (**2b**)

	x	*y*	*z*	*U*(eq)[a]
Os(1)	2718.7(4)	5770.2(4)	4612.1(3)	17.9(1)
Os(2)	3889.2(4)	3760.4(3)	4532.1(2)	15.4(1)
Os(3)	3969.4(5)	5198.7(4)	3226.4(2)	17.4(1)
Os(4)	6084.0(4)	4745.2(3)	4113.6(2)	15.0(1)
P(1)	4711(3)	5445(2)	4964(2)	15.6(8)
O(1)	2622(11)	8225(8)	4535(7)	48(4)
O(2)	188(9)	5314(9)	3992(6)	43(4)
O(3)	1814(9)	5667(10)	6184(6)	42(4)
O(4)	1357(9)	2967(8)	4172(6)	38(3)
O(5)	5351(10)	1752(7)	4111(6)	38(3)
O(6)	3694(10)	2837(7)	6078(5)	32(3)
O(7)	3366(11)	2867(8)	2715(5)	42(4)
O(8)	4782(9)	7554(7)	3566(6)	33(3)
O(9)	1664(9)	6009(9)	2467(6)	44(4)
O(10)	5735(10)	5248(9)	1929(5)	41(3)
O(11)	6751(9)	3106(7)	2900(5)	28(3)
O(12)	7572(9)	6628(9)	3567(6)	36(3)
O(13)	8091(9)	4187(8)	5204(6)	36(3)
C(1)	2633(12)	7280(11)	4566(8)	30(4)
C(2)	1142(15)	5466(11)	4211(7)	33(4)
C(3)	2133(11)	5727(11)	5590(8)	26(4)
C(4)	2307(14)	3264(10)	4325(7)	30(4)
C(5)	4802(11)	2520(10)	4257(7)	23(4)
C(6)	3770(11)	3195(9)	5492(7)	23(3)
C(7)	3562(13)	3690(12)	2939(7)	31(4)
C(8)	4485(13)	6681(11)	3488(7)	25(4)
C(9)	2488(12)	5697(11)	2762(7)	27(4)
C(10)	5050(14)	5213(11)	2400(7)	28(4)
C(11)	6540(10)	3701(10)	3326(7)	21(3)
C(12)	7028(11)	5909(11)	3763(7)	24(4)
C(13)	7344(12)	4406(10)	4804(8)	29(4)
C(14)	5097(10)	5604(9)	5957(6)	15(3)
C(15)	5729(11)	4889(11)	6350(6)	24(3)
C(16)	6027(14)	5037(12)	7089(7)	37(4)
C(17)	5608(12)	6000(15)	7416(8)	42(5)
C(18)	4992(17)	6758(12)	7014(8)	44(5)
C(19)	4736(12)	6567(11)	6283(7)	27(4)

[a] Equivalent isotropic *U* defined as one-third of the trace of the orthogonalized U_{ij} tensor.

Table IV. Selected Interatomic Bond Distances (Å) and Angles (deg) for $M_4(CO)_{13}(\mu_3\text{-PPh})$ (M = Ru (**2a**), Os (**2b**))

bond dist/angle	**2a**	**3b**
M(1)–M(2)	2.792(1)	2.802(1)
M(1)–M(3)	2.929(1)	2.947(1)
M(2)–M(3)	2.941(1)	2.955(1)
M(2)–M(4)	2.816(1)	2.817(1)
M(3)–M(4)	2.856(1)	2.890(1)
M(1)–P(1)	2.309(1)	2.328(3)
M(2)–P(1)	2.374(1)	2.400(3)
M(4)–P(1)	2.302(1)	2.327(3)
M(2)–M(1)–M(3)	61.8(1)	61.8(1)
M(1)–M(2)–M(4)	91.5(1)	91.7(1)
M(1)–M(2)–M(3)	61.4(1)	61.5(1)
M(3)–M(2)–M(4)	59.4(1)	60.0(1)
M(1)–M(3)–M(2)	56.8(1)	56.7(1)
M(1)–M(3)–M(4)	88.0(1)	87.4(1)
M(2)–M(3)–M(4)	58.1(1)	57.6(1)
M(2)–M(4)–M(3)	62.5(1)	62.3(1)
M(3)–M(1)–P(1)	74.3(1)	75.4(1)
M(1)–M(2)–P(1)	52.4(1)	52.5(1)
M(3)–M(2)–P(1)	73.2(1)	74.2(1)
M(4)–M(2)–P(1)	51.8(1)	52.2(1)
M(2)–M(4)–P(1)	54.1(1)	54.6(1)
M(3)–M(4)–P(1)	75.9(1)	76.5(1)
M(1)–P(1)–M(2)	73.2(1)	72.7(1)
M(1)–P(1)–M(4)	121.2(1)	120.0(1)
M(2)–P(1)–M(4)	74.1(1)	73.2(1)
P(1)–M(1)–C(1)	104.4(1)	103.0(4)
P(1)–M(1)–C(2)	156.7(1)	157.8(4)
P(1)–M(1)–C(3)	93.2(1)	93.7(4)
P(1)–M(2)–C(4)	134.5(1)	134.0(4)
P(1)–M(2)–C(5)	122.2(1)	125.6(4)
P(1)–M(2)–C(6)	91.3(1)	92.7(4)
P(1)–M(4)–C(11)	151.0(1)	151.7(3)
P(1)–M(4)–C(12)	107.0(1)	107.5(4)
P(1)–M(4)–C(13)	97.3(1)	97.2(4)

restrictions upon the reaction conditions employed to initiate reactions. There is considerable interest in the butterfly class of tetranuclear clusters displaying a nonplanar arrangement of metal atoms.[10,11] Such clusters often bear small molecules or main group atoms within the cavity between the wing tip atoms and exhibit unusual reactivity patterns.[28] The intracavity coordination environment of butterfly clusters is flexible and facilitates small-molecule activation through multisite coordination.[29] We recently established an extensive manifold of chemistry for the phosphinidene-stabilized butterfly cluster *nido*-$Ru_4(CO)_{13}(\mu_3\text{-PPh})$ (**2a**), containing a butterfly configuration of metal atoms, and reported a remarkably facile activation of dihydrogen by **2a**, which occurs upon UV irradiation under ambient conditions.[30] We have also noted that the arrangement of metal atoms in this skeletal framework bears a close similarity to the metal atom connectivity at a stepped catalytically active site of a close-packed array of metal atoms.

In order to fully develop the potential chemistry of this remarkable cluster, we have designed a synthetic procedure allowing its preparation in workable quantities. A similar methodology is readily extendable to the osmium analogue. Clusters **2a** and **2b** possess μ_3-phosphinidene ligands and display a remarkable resistance to fragmentation. Indeed, it appears that in many instances the μ_3-phosphinidene fragment appears to act as an integral part of the skeletal framework, adopting the role of a skeletal atom and, in several instances, facilitating coordination. There are few reports of this activating influence of main group elements on clusters.[31]

1. Syntheses. (a) Strategy. A convenient preparation of **2a** involves reductive elimination of benzene and a condensation reaction of $HRu_3(CO)_{10}(\mu\text{-}PPh_2)$ (**1a**) (eqs 1–3). The catalyzed substitution of carbon monoxide for diphenylphosphine in dodecacarbonyltriruthenium affords $Ru_3(CO)_{11}(PPh_2H)$ (I) essentially quantitatively.[32] **1a** is readily obtained by gentle thermolysis (55 °C, 12 h), which initiates decarbonylation and oxidative addition of P–H to the cluster. Formation of the decacarbonyl

(28) (a) Dahl, L. F.; Smith, D. L. *J. Am. Chem. Soc.* **1962**, *84*, 2450. (b) Gervasio, G.; Rossetti, R.; Stanghellini, P. L. *Organometallics* **1985**, *4*, 1612. (c) Rumin, R.; Robin, F.; Petillon, F. Y.; Muir, K. W.; Stevenson, I. *Organometallics* **1991**, *10*, 2274. (d) Sappa, E.; Belletti, D.; Tiripicchio, A.; Tiripicchio-Camellini, M. *J. Organomet. Chem.* **1989**, *359*, 419. (e) Lentz, D.; Micheal, H. *Angew. Chem., Int. Ed. Engl.* **1988**, *100*, 871. (f) Albiez, T.; Powell, A. K.; Vahrenkamp, H. *Chem. Ber.* **1990**, *123*, 667. (g) Bantel, H.; Powell, A. K.; Vahrenkamp, H. *Chem. Ber.* **1990**, *123*, 661. (h) Collins, M. A.; Johnson, B. F. G.; Lewis, L.; Mace, J. M.; Morris, J.; McPartlin, M.; Nelson, W. J. H.; Puga, J.; Raithby, P. R. *J. Chem. Soc., Chem. Commun.* **1983**, *689*. (i) Blohm, M. L.; Gladfelter, W. L. *Organometallics* **1985**, *4*, 45. (j) Cowie, A. G.; Johnson, B. F. G.; Lewis, J.; Raithby, P. R. *J. Organomet. Chem.* **1988**, *306*, C63. (k) Holt, E. M.; Whitmire, K. H.; Shriver, D. F. *J. Organomet. Chem.* **1981**, *213*, 125. (l) Adams, R. D.; Babin, J. E.; Tanner, J. T. *Organometallics* **1988**, *7*, 765.

(29) (a) Horwitz, C. P.; Shriver, D. F. *Adv. Organomet. Chem.* **1984**, *23*, 219. (b) Shriver, D. F.; Sailor, M. J. *Acc. Chem. Res.* **1988**, *21*, 374.

(30) van Gastel, F.; Corrigan, J. F.; Doherty, S.; Taylor, N. J.; Carty, A. J. *Inorg. Chem.* **1992**, *31*, 4492.

(31) (a) Adams, R. D.; Wang, S. *Organometallics* **1985**, *4*, 1902. (b) Adams, R. D.; Wang, S. *Organometallics* **1986**, *5*, 1274. (c) Adams, R. D.; Wang, S. *J. Am. Chem. Soc.* **1987**, *109*, 924. (d) Adams, R. D.; Wang, S. *Organometallics* **1987**, *7*, 739. (e) Eber, B.; Buchholz, D.; Huttner, G.; Fässler, T.; Imhof, W.; Fritz, M.; Daran, J. C.; Jeannin, Y. J. *Organomet. Chem.* **1991**, *401*, 49. (f) Hansert, B.; Powell, A. K.; Vahrenkamp, H. *Chem. Ber.* **1991**, *124*, 2697. (g) Knoll, K.; Fässler, T.; Huttner, G. *J. Organomet. Chem.* **1987**, *332*, 309. (h) Song, J.-S.; Han, S. H.; Nguyen, S. T.; Geoffroy, G. L.; Rheingold, A. L. *Organometallics* **1990**, *9*, 2385. (i) Song, J.-S.; Geoffroy, G. L.; Rheingold, A. L. *Inorg. Chem.* **1992**, *31*, 1505.

(32) (a) van Gastel, F. Ph.D. Thesis, University of Waterloo, 1991. (b) The ketyl route to $Ru_3(CO)_{11}(PR_3)$ derivatives was first described by Bruce and co-workers: Bruce, M. I.; Kehoe, D. C.; Matisons, J. G.; Nicholson, B. K.; Rieger, P. H.; Williams, M. L. *J. Chem. Soc., Chem. Commun.* **1982**, 442.

$$Ru_3(CO)_{12} \xrightarrow[PPh_2H]{Na/Ph_2CO^{\bullet}, THF} Ru_3(CO)_{11}(PPh_2H) \quad \mathbf{I} \qquad (1)$$

$$Ru_3(CO)_{11}(PPh_2H) \xrightarrow[12\ h]{hexane,\ 50\ ^\circ C} (\mu\text{-H})Ru_3(CO)_{10}(\mu\text{-PPh}_2) \quad \mathbf{1a} \qquad (2)$$

$$(\mu\text{-H})Ru_3(CO)_{10}(\mu\text{-PPh}_2) \xrightarrow[-C_6H_6]{toluene,\ 110\ ^\circ C} Ru_4(CO)_{13}(\mu_3\text{-PPh}) \quad \mathbf{2a} \qquad (3)$$

compound is accompanied by varying quantities of the unsaturated cluster $HRu_3(CO)_9(\mu\text{-PPh}_2)$ (**3**). We have discovered that the yields of **2a** are not dependent upon the relative proportions of **1a** and **3** in the initial reaction solution. Heating a concentrated toluene solution of **1a/3** at reflux and simultaneously purging with a steady stream of carbon monoxide afforded $Ru_4(CO)_{13}(\mu_3\text{-PPh})$ (**2a**) in workable quantities after chromatographic workup. Several condensation products of higher nuclearity were also identified in the reaction mixture and have been previously described. These include dark green $Ru_5(CO)_{15}(\mu_4\text{-PPh})$,[19] green/brown $(\mu_3\text{-H})Ru_5(CO)_{13}(\mu_4\text{-PPh})(\mu\text{-PPh}_2)$,[22] and two clusters of nuclearity 7 and 8: deep green $Ru_7(CO_{18}(\mu_4\text{-PPh})_2$[23] and dark brown $Ru_8(CO)_{21}(\mu_6\text{-P})(\mu_4\text{-PPh})(\mu_2\text{-PPh}_2)$.[24] The compounds $Ru_3(CO)_{12}$ and a mixture of $(\mu\text{-H})_2Ru_3(CO)_8(\mu\text{-PPh}_2)_2$[20] and $Ru_2(CO)_6(\mu\text{-PPh}_2)_2$[21] were also isolated as side products.

Heating a toluene solution of **1a** at reflux in the absence of carbon monoxide resulted in more rapid formation of $Ru_4(CO)_{13}(\mu_3\text{-PPh})$ (**2a**), complete conversion requiring only 1 h with essentially similar yields. Such a rate enhancement in the absence of coordinating CO suggests that formation of **2a** proceeds through the unsaturated cluster $(\mu\text{-H})Ru_3(CO)_9(\mu\text{-PPh}_2)$ (**3**).[33] A single-crystal X-ray analysis of **3** has shown that the endo phenyl ring of the phosphido ligand participates in a weak η^2-interaction of its P–C(Ph) bond with the unsaturated ruthenium center. This secondary interaction may lead to P–C activation and cleavage via reductive elimination of benzene. As yet, we are unsure whether formation of **2a** proceeds through the unsaturated cluster $Ru_3(CO)_9(\mu_3\text{-PPh})$ (**4**) (i.e. elimination of C_6H_6 prior to coordination of a metal fragment) or by cluster condensation forming a tetranuclear cluster, followed by rapid elimination of benzene Scheme I (vide infra).

(b) Preparation of $Ru_4(CO)_{13}(\mu_3\text{-PPh})$ from $[Ru_4(CO)_{13}]^{2-}$. We have developed an alternative procedure for the preparation of *nido*-$Ru_4(CO)_{13}(\mu_3\text{-PPh})$ which enables the synthesis to be extended to phosphinidene-functionalized analogues of **2a**. Cluster **2a** can be prepared as described in eq 4. The dianion $[Ru_4(CO)_{13}]^{2-}$ is readily available by reduction of dodecacarbonyltriruthenium with potassium,[18] proceeding quantitatively to yield a deep red homogeneous solution to which dichlorophen-

$$K_2[Ru_4(CO)_{13}] \xrightarrow[3\ h]{PPhCl_2,\ THF} Ru_4(CO)_{13}(\mu_3\text{-PPh}) \qquad (4)$$

ylphosphine can be added to afford the required product, **2a**. We have successfully applied a similar procedure to the preparation of other butterfly clusters containing μ_2-phosphido bridges by reaction with the appropriate monochlorophosphine.[34] Although the yields obtained using this procedure are not as good as those from the pyrolysis sequence, the latter method has two distinct advantages: (i) there is a reduction in preparation time and (ii)

Scheme I

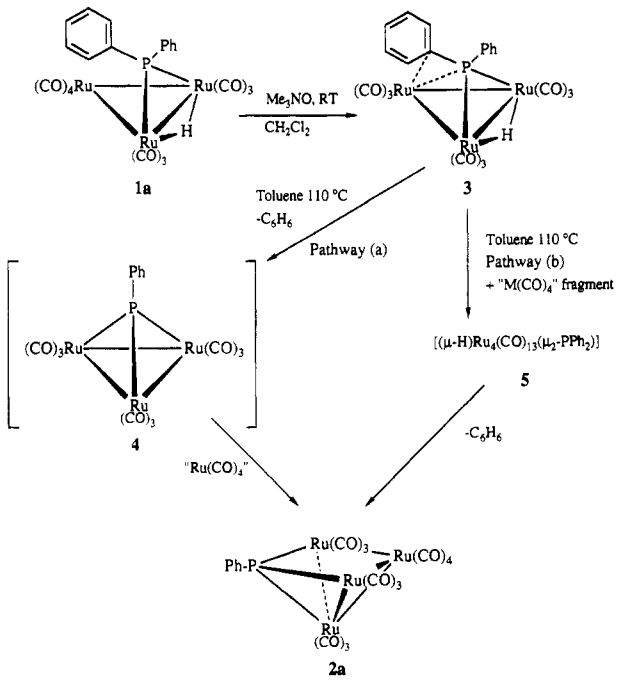

the methodology can easily be extended to tailor the phosphinidene ligand, $RPCl_2$, and vary the steric and electronic properties of the R group.

The $^{31}P\{^1H\}$ NMR spectrum of **2a** consists of a single resonance at δ 409 ppm characteristic of a μ_3-phosphinidene fragment.[35] We have found this ^{31}P shift to be a useful spectroscopic tool for providing structural information. When the Ru_4P skeletal structure is retained, the ^{31}P shift is almost invariant. On the other hand, structural rearrangement at the phosphorus ligand, i.e. P–C bond formation,[11] skeletal atom isomerization,[14] and the formation of clusters with unusual electron counts, results in dramatic upfield ^{31}P shifts.[36] The $^{13}C\{^1H\}$ NMR spectrum of **2a** contains the expected four resonances associated with the phosphorus-bound phenyl ring. However the carbonyl region of the spectrum displays two broad resonances, indicating that a facile carbonyl-exchange process is occurring. This was subsequently confirmed by a variable-temperature NMR study (vide infra).

(c) Synthesis of $Os_4(CO)_{13}(\mu_3\text{-PPh})$. The successful preparation of **2a** from $HRu_3(CO)_{10}(\mu\text{-PPh}_2)$ (**1a**) prompted us to investigate the potential of the osmium congener to form the corresponding cluster $Os_4(CO)_{13}(\mu_3\text{-PPh})$ (**2b**) via a similar procedure. The quantitative formation of $(\mu\text{-H})Os_3(CO)_{10}(\mu\text{-PPh}_2)$ (**1b**) from dodecacarbonyltriosmium has previously been reported by Lewis and co-workers.[16]

Heating a xylene solution of **1b** at reflux failed to give the desired product **2b**, affording only $(\mu\text{-H})_2Os_3(CO)_9\{\mu\text{-P(Ph)}C_6H_4\}$ (**6**) in high yield. Heating a solid sample of **1b** in a sealed Schlenk tube at 215 °C for 8 min led to the isolation of $Os_4(CO)_{13}(\mu_3\text{-PPh})$ (**2b**) (21%) after chromatographic purification. Cluster **6** was isolated as a minor product from the reaction mixture. Reduced reaction temperatures provided higher proportions of metalated **6** at the expense of **2b**, indicating the possible intermediacy of **6**. This proposal was unequivocally established by independently preparing a sample of $(\mu\text{-H})_2Os_3(CO)_9\{\mu\text{-}$

(33) MacLaughlin, S. A.; Carty, A. J.; Taylor, N. *J. Can. J. Chem.* **1982**, *60*, 87.
(34) Corrigan, J. F.; Doherty, S.; DiNardo, M.; Taylor, N. J.; Carty, A. J. *J. Cluster Sci.*, in press.
(35) Carty, A. J.; MacLaughlin, S. A.; Nucciarone, D. In *Phosphorus-13 NMR Spectroscopy in Stereochemical Analysis*: Organic Compounds and Metal Complexes; Verkade, J. G., Quinn, L. D., Eds.; VCH Publishers, Inc.: New York, 1987, Chapter 16, pp 539–619.
(36) van Gastel, F.; Agocs, L.; Cherkas, A. A.; Corrigan, J. F.; Doherty S.; Ramachandran, R.; Taylor, N. J.; Carty, A. J. *J. Cluster Sci.* **1991**, *2*, 131.

Scheme II

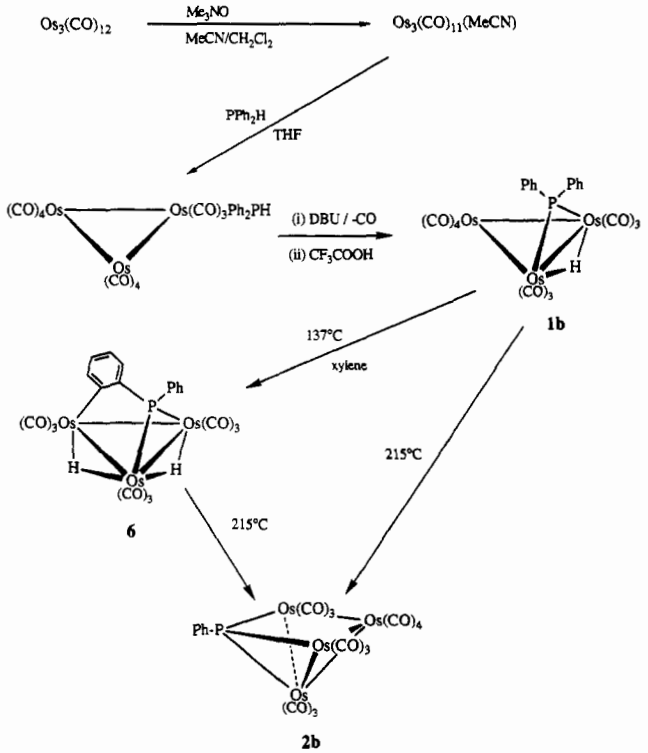

$P(Ph)C_6H_4\}$ (**6**) and converting it to **2b** under conditions similar to those described above. Scheme II summarizes these observations.

Several contrasting features between the formation of **2a** and **2b** can be noted: (i) $(\mu\text{-H})_2Os_3(CO)_9\{\mu\text{-P(Ph)}C_6H_4\}$ (**6**) is isolated as an intermediate in the formation of **2b**. There is no evidence for the formation of an analogous ruthenium-containing species in the preparation of **2a**. (ii) The coordinatively and electronically unsaturated $(\mu\text{-H})Ru_3(CO)_9(\mu\text{-PPh}_2)$ (**3**) is an intermediate in the formation of **2a**. We found no evidence for a similar osmium analogue. This latter observation suggests that orthometalation is not a prerequisite for P–C bond cleavage but that interaction of this bond with the unsaturated metal center is sufficient to initiate activation. Observation (i) suggests that orthometalation may provide an additional pathway for the elimination of benzene.

2. Mechanistic Implications. We have so far been unable to establish the intermediacy of the unsaturated 46-electron cluster $Ru_3(CO)_9(\mu_3\text{-PPh})$ (**4**) (i.e. intramolecular elimination of benzene from **3**) although, in the presence of dihydrogen, $(\mu\text{-H})Ru_3(CO)_9(\mu\text{-PPh}_2)$ (**1a**) forms $(\mu\text{-H})_2Ru_3(CO)_9(\mu_3\text{-PPh})$.[33] This may reflect the requirement that **1a** add dihydrogen prior to P–C bond cleavage while formation of **2a** requires an additional metal fragment to initiate loss of benzene. In support of this proposal, it has been shown that both $(\mu\text{-H})Ru_3(CO)_9(\mu\text{-PPh}_2)$ (**3**)[33] and $(\mu\text{-H})_2Os_3(CO)_9\{\mu\text{-P(Ph)}C_6H_4\}$ (**6**)[37] behave similarly toward H_2, forming $(\mu\text{-H})_2M_3(CO)_9(\mu_3\text{-PPh})$ (M = Ru, Os). Both clusters possess the capacity to associatively add incoming reagents. For **3** the presence of a coordinatively unsaturated $Ru(CO)_3$ fragment facilitates addition,[38] while for **6** reversible metalation[25] provides a similar site for the addition of H_2 prior to P–C bond cleavage. Thus addition of an extra metal fragment may be a prerequisite for the reductive elimination of benzene from **3**. We can therefore differentiate two mechanistic pathways: (a) intramolecular elimination of benzene and formation of "$Ru_3(CO)_9(\mu_3\text{-PPh})$" (**4**) and (b) condensation of a metal fragment with **3** and the intermediacy of a species $(\mu\text{-H})Ru_4(CO)_{13}(\mu\text{-PPh}_2)$ **5** followed by P–C cleavage (Scheme I).

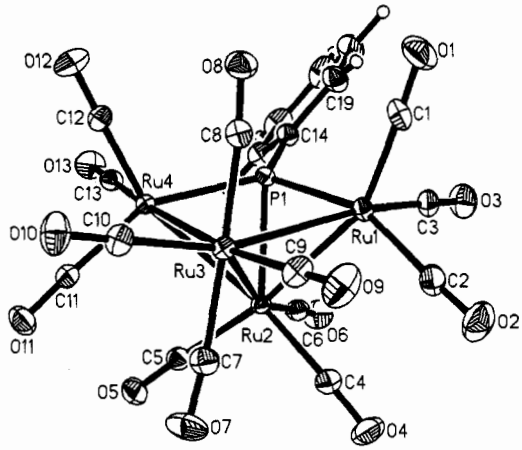

Figure 1. Perspective view of the molecular structure of *nido*-$Ru_4(CO)_{13}(\mu_3\text{-PPh})$ (**2a**) illustrating its square pyramidal geometry containing an Ru_3P square base.

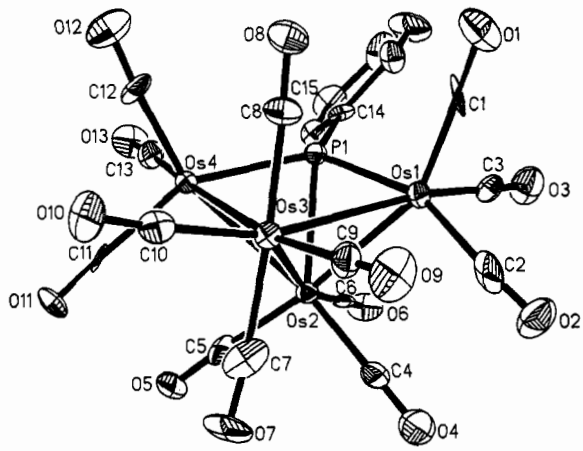

Figure 2. Perspective view of the molecular structure of *nido*-$Os_4(CO)_{13}(\mu_3\text{-PPh})$ (**2b**) in an orientation similar to that of **2a** illustrated in Figure 1.

3. X-ray Structures of $M_4(CO)_{13}(\mu_3\text{-PPh})$ (M = Ru (2a), Os (2b)). The molecular structures of **2a** and **2b** are shown in Figures 1 and 2, respectively, with a selection of bond distances and angles given in Table II. Crystals of **2a** and **2b** are isomorphous, crystallizing in the orthorhombic space group $P2_12_12_1$. The skeletal framework contains a butterfly arrangement of metal atoms, consistent with a 62-electron count and current bonding theories.[39] The phosphinidene ligand caps an open triangular face bonded to both wing tip atoms and a hinge metal atom affording a five-vertex polyhedron described as a nido octahedron containing a "PPh" fragment occupying a basal vertex. Each cluster contains an $M(CO)_4$ unit in the basal plane, the remaining metal atom vertices each being bonded to three carbonyl ligands. The dihedral angles between the two wings of the butterfly are 110.9 and 110.6° for **2a** and **2b**, respectively, within the range expected for electron-precise butterfly clusters supporting main group fragments between the wing tip atoms.[13,40] The longest metal–metal bonds within these clusters are those between the hinge metal atoms [Ru(2)–Ru(3) = 2.941(1) Å, Os(2)–Os(3) = 2.955(1) Å] with the remaining bonding distances falling in the

(37) Colbran, S. B.; Irele, P. T.; Johnson, B. F. G.; Kaye, P. T.; Lewis, J.; Raithby, P. R. *J. Chem. Soc., Dalton Trans.* **1989**, 2033.

(38) (a) Carty, A. J.; MacLaughlin, S. A.; Taylor, N. J. *Organometallics* **1983**, *2*, 1194. (b) van Gastel, F.; MacLaughlin, S. A.; Lynch, M.; Carty, A. J.; Sappa, E.; Tiripicchio, A.; Tiripicchio-Camellini, M. *J. Organomet. Chem.* **1987**, *326*, C65.

(39) (a) Mingos, D. M. P.; May, A. S. In *The Chemistry of Metal Cluster Complexes*; Shriver, D. F., Kaesz, H. D., Adams, R. D., Eds.; VCH Publishers, Inc: New York, 1990. (b) Mingos, D. M. P.; Wales, D. J. In *Introduction to Cluster Chemistry*; Grimes, R. N., Ed.; Prentice Hall, Inc: Englewood Cliffs, NJ, 1990.

(40) Fjare, D. E.; Jensen, J. A.; Gladfelter, W. L. *Inorg. Chem.* **1983**, *22*, 1774.

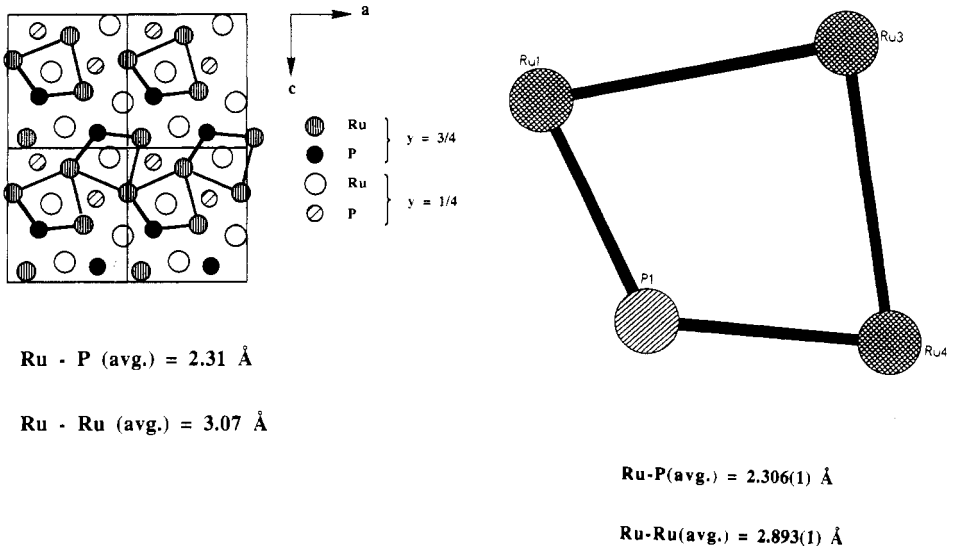

Figure 3. Comparison of ruthenium–ruthenium and ruthenium–phosphorus connectivities in (left) the Ru_3P units of Ru_2P (010) and (right) the Ru_3P square face of **2a**.

ranges 2.792(1)–2.929(1) Å for **2a** and 2.802(1)–2.947(1) Å for **2b**. Neglecting the rotation of the phenyl ring about P(1)–Ru(4), there is an approximate mirror plane passing through Ru(2), Ru(3), and P(1). The μ_3-phosphinidene fragment symmetrically caps the wing tip metal atoms M(1) and M(2) [Ru(1)–P(1) = 2.309(1) Å, Ru(4)–P(1) = 2.302(1) Å; Os(1)–P(1) = 2.328(1) Å, Os(4)–P(1) = 2.327(1) Å], with the metal–phosphorus bond to the hinge being marginally longer [Ru(2)–P(1) = 2.374(1) Å, Os(2)–P(1) = 2.400(1) Å]. The longer Os–P distances simply reflect the larger atomic radius of the heavier congener, though within the individual structures there are no unusual M–P bonding distances for a 62-electron phosphinidene-stabilized cluster. The M–P bonding distances are longer than those described for μ_3-phosphinidene ligands capping closed M_3 triangular faces,[41] more closely resembling those of a capped open triangular array.[42]

Finally, the M(4), M(3), M(1), and P(1) atoms of **2a** and **2b** define a square planar arrangement of skeletal vertices, but the rectangle has a severely distorted geometry due to the vastly disparate sizes of the two different nuclei [Ru–Ru(av) = 2.893(1) Å, Os–Os(av) = 2.919(1) Å; Ru–P(av) = 2.306(1) Å, Os–P(av) = 2.328(1) Å]. The atoms M(1), M(3), M(4), and P(1) are approximately coplanar, with the greatest deviation from the best least-squares plane being +0.0628 Å (P(1)) and +0.0838 Å (P(1)) for **2a** and **2b**, respectively. The axial carbonyl C(8)O(8) directed above the Ru_3P square plane is distorted toward P(1) [Ru(3)–C(8)–O(8) = 171.1(1)°]. This is reflected in the exceptionally acute angle associated with P(1)–Ru(3)–C(8) [67.9(1)°], carbonyls C(7)O(7) and C(8)O(8) retaining a trans disposition [C(7)–Ru(3)–C(8) = 176.1(1)°]. The carbonyl C(8)O(8) in **2b** exhibits a similar distortion [P(1)–Os(3)–C(8) = 67.1(4)°, Os(3)–C(8)–O(8) = 173.2(12)°, C(7)–Os(3)–C(8) = 176.2(6)°].

4. $Ru_4(CO)_{13}(\mu_3$-PPh) as a Molecular Model for Metal and Mixed Main Group–Metal Surfaces. The Ru_3P bonding arrangement contained in the basal plane of **2a** bears a remarkably close similarity to the atom connectivity found in ruthenium phosphide, Ru_2P, in the (010) plane. Figure 3 shows the close resemblance of the phosphorus and ruthenium connectivity in Ru_2P to that of Ru(1), Ru(3), Ru(4), and P(1) in **2a**. Ru_2P has a *C*23 ($PbCl_2$) type structure, and the structure of Fe_2P is not greatly different. In both structures, the P atoms are 9-fold coordinated by the metal atoms in a tetrakaidecahedral arrangement. There is also a close similarity in the Ru–P and Ru–Ru bonding distances within the Ru_3P units of ruthenium phosphide and this potential molecular model [**2a**, Ru–P(av) = 2.306(1) Å, Ru–Ru(av) = 2.893(1) Å; Ru_2P, Ru–P(av) = 2.31 Å, Ru–Ru(av) = 3.07 Å]. Conversely, a simple skeletal rearrangement of **2a** to a framework containing an Ru_4 basal plane would resemble the arrangement of metal atoms in ruthenium metal (100). It has been suggested that the coordination of benzene on a square or rectangular Ru_4 fragment could be a model for the dissociative chemisorption of benzene at ruthenium metal.[2] In fact, the Ru(100) plane of Ru metal contains two markedly different Ru–Ru contacts [Ru–Ru(short) = 2.70 Å and Ru–Ru(long) = 4.28 Å].[43] Such an array of metal atoms might better be approximated by two metal–metal-bonded dimers held in close proximity by weak secondary interactions between the metals. We are as yet unaware of a cluster that could accurately mimic such an atom connectivity, but the potential topological analogy drawn between this metal cluster and Ru_4 surface-absorbate complexes could still prove to be informative.[3a]

We have recently shown that the nido skeletal famework of **2a** readily undergoes isomerization upon coordination of small molecules to a square Ru_4 array. Such Ru_4 derivatives may serve as models for the chemisorption of small unsaturated hydrocarbons on an Ru_4 surface. The capacity to prepare **2a** in workable quantities, coupled with its high thermal and photochemical stability and its diverse reactivity, often under exceptionally mild conditions, offers a potentially attractive model for evaluating processes occurring either at a catalytically active site of a stepped metal surface (small molecule chemisorption, C-X activation/cleavage) or at a mixed main group–metal surface. Furthermore the process of skeletal transformation to afford a planar Ru_4 face merits an in depth investigation into its chemistry to support the proposal that such an array of metal atoms does model a metallic ruthenium surface.

5. $^{13}C\{^1H\}$ NMR Studies of $Ru_4(CO)_{13}(\mu_3$-PPh). A representative set of $^{13}C\{^1H\}$ NMR spectra from 196 to 348 K are illustrated in Figure 4 revealing the dynamic behavior associated with **2a**. We have previously described the carbonyl-exchange processes occurring in $(\mu\text{-H})_2Ru_4(CO)_{12}(\mu_3\text{-PPh})$,[30] and a direct comparison will be made with the exchange in $Ru_4(CO)_{13}(\mu_3$-

(41) (a) Deeming, A. J.; Doherty, S.; Powell, N. I. *Inorg. Chim. Acta* **1992**, *198–200*, 469. (b) Iwasaki, F.; Mays, M. J.; Raithby, P. R.; Taylor, P. L.; Wheatley, P. J. *J. Organomet. Chem.* **1981**, *213*, 185. (c) Natarajan, K.; Scheidsteger, O.; Huttner, G. *J. Organomet. Chem.* **1981**, *221*, 301. (d) Bruce, M. I.; Horn, E.; Shawkataly, O. B.; Snow, M. R.; Tiekink, E. R. J.; Williams, M. L. *J. Organomet. Chem.* **1986**, *316*, 187.

(42) Field, J. S.; Haines, R. J.; Smit, D. N. *J. Organomet. Chem.* **1982**, *240*, C23.

(43) Emsley, J. *The Elements*; Oxford University Press: New York, 1991, pp 166–7.

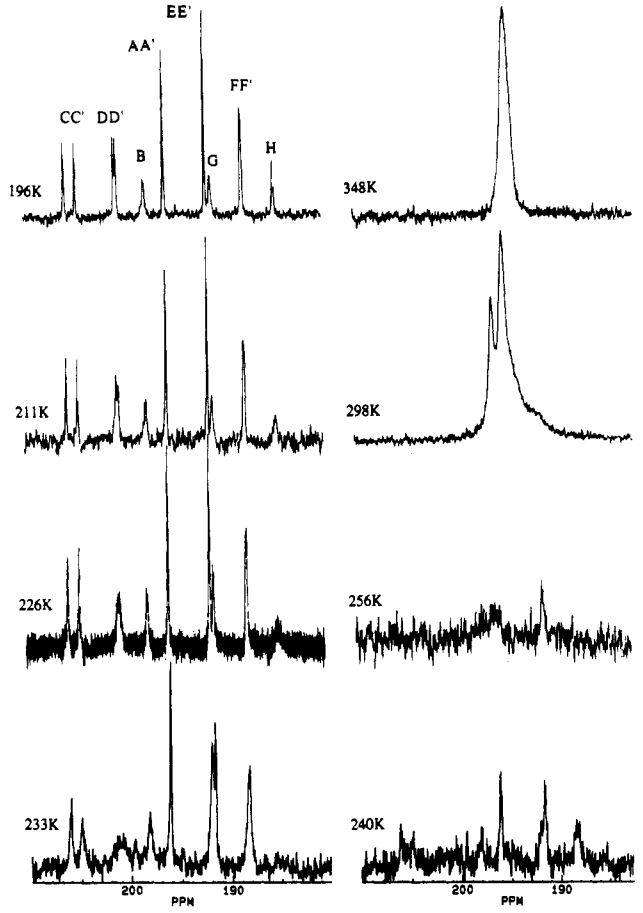

Figure 4. Variable-temperature $^{13}C\{^1H\}$ NMR spectra of *nido*-$Ru_4(CO)_{13}(\mu_3$-PPh) (**2a**) in the carbonyl region.

PPh). The eight unique carbonyl sites of **2a** are labeled as shown in Figure 5 and are consistent with that used for $(\mu$-$H)_2Ru_4(CO)_{12}(\mu_3$-PPh). Cluster **2a** contains a pseudomirror plane passing through Ru(2), Ru(3), and P(1), and this is reflected in the low-temperature $^{13}C\{^1H\}$ NMR spectrum. At 196 K, eight sharp resonances have been identified (δ 205.2, 200.7, 197.8, 195.8, 191.7, 191.1, 187.8, 184.9), suggesting the the slow-exchange limit has been reached. In comparison, the carbonyl ligands in $(\mu$-$H)_2Ru_4(CO)_{12}(\mu_3$-PPh) are not all static, a facile trigonal rotation at Ru(2) occurring at the lowest temperatures accessible. Despite this difference, there are several informative similarities and a comparison of the low-temperature $^{13}C\{^1H\}$ NMR spectrum of **2a** with that of $(\mu$-$H)_2Ru_4(CO)_{12}(\mu_3$-PPh) coupled with the evolution of its resonances with increasing temperature allowed a consistent assignment of each individual ^{13}CO resonance. The resonance at δ 205.2 shows the largest coupling to phosphorus ($^2J_{PC}$ = 70.4 Hz) characteristic of a carbonyl trans to phosphorus (CC'), i.e. C(2)O(2) and C(11)O(11) [P(1)–Ru(1)–C(1) = 156.7(1)°, P(1)–Ru(4)–C(11) = 151.0(1)°]. The signal at δ 195.8 (singlet) associated with two equivalent carbonyl ligands has a chemical shift similar to those unequivocally assigned to AA' in $(\mu$-$H)_2Ru_4(CO)_{12}(\mu_3$-PPh).[30,44] This single resonance is assigned to the carbonyl ligands bound to Ru(3) [C(10)O(10) and C(9)O(9)]. An examination of the NMR spectrum in the temperature range 196–234 K revealed that with increasing temperature the first carbonyl ligands to undergo exchange were those associated with the resonances at δ 200.7 (intensity 2) and 184.9 (intensity 1). This low-energy exchange process is similar to that observed in $(\mu$-$H)_2Ru_4(CO)_{12}(\mu_3$-PPh),

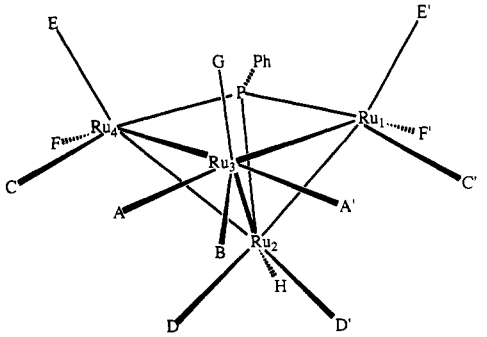

Figure 5. Carbonyl-labeling scheme used for *nido*-$Ru_4(CO)_{13}(\mu_3$-PPh) (**2a**).

and we can confidently assign the low-field signal to DD' and the high field one to H, the associated process being rapid trigonal rotation. The resonances at δ 205.2 (already assigned to CC'), 191.7, and 187.7 all began to show simultaneous exchange broadening in the temperature range 226–243 K. By analogy with the carbonyl ligand assignment in $(\mu$-$H)_2Ru_4(CO)_{12}(\mu_3$-PPh) and the close similarity of the exchange processes, the two unassigned resonances must belong to the four remaining wing tip carbonyl ligands. The signal at δ 187.7 showed coupling to ^{31}P [$^2J_{PC}$ = 9.5 Hz]. We attribute this resonance to the carbonyl occupying site FF' (Figure 5). The remaining carbonyl resonance (δ 191.7) must therefore be due to CO groups occupying sites EE' [C(1)O(1) and C(12)O(12)], further substantiating the proposal of an angular dependence of $^2J_{PC}$.[45] This also suggests a nearly zero J value for P–M–C angles close to 110° [P(1)–Ru(1)–C(3) = 93.2(1)°, P(1)–Ru(4)–C(13) = 97.3° for FF'; P(1)–Ru(1)–C(1) = 104.4(1)°, P(1)–Ru(4)–C(12) = 107.0(1)° for EE']. Finally, the resonances at δ 195.8 and 197.8 start to exchange at higher temperature (above 234 K), while at 240 K the only carbonyl not to exhibit exchange broadening is that appearing at δ 191.1. The presence of a similar higher energy trigonal rotation was noted in the dynamic behavior of $(\mu$-$H)_2Ru_4(CO)_{12}(\mu_3$-PPh) and was assigned to rotation occurring at the bridgehead ruthenium atom of the two hydride ligands. Although the equivalent exchange process occurs at far lower temperatures in **2a**, we can confidently assign the signals at δ 195.8 and 197.8 to carbonyls B and AA', respectively, while the remaining sharp resonance (δ 191.1) must be that of the fourth carbonyl ligand attached to Ru(3). A higher energy carbonyl exchange at metal centers, the result of the presence of attached hydride ligands, is not unusual, and our observations simply confirm this well-documented process. Raising the temperature still further induces broadening of the final carbonyl signal. These latter exchange processes are characteristic of carbonyl exchange in an $Ru(CO)_4$ fragment: first a lower energy 3-fold rotation[46] and finally exchange of the fourth CO group possibly via two consecutive trigonal rotations. Above room temperature, line broadening indicates the onset of facile intermetallic carbonyl scrambling, a process not previously observed for $(\mu$-$H)_2Ru_4(CO)_{12}(\mu_3$-PPh), since significant decomposition above 20 °C limited the temperature range accessible. However, total carbonyl scrambling ($T \geq 340$ K) has been observed in the related heterometallic cluster $(\mu$-$H)_2RuOs_3(CO)_{12}(\mu_3$-$PC_6H_{11})$, in which the unique ruthenium atom occupies a wingtip position.[47]

We have identified five distinct carbonyl exchange processes in **2a**. The first and lowest energy process is associated with trigonal rotation at Ru(2). Unlike the associated process in (μ-

(44) Blohm, M. L.; Fjare, D. E.; Gladfelter, W. L. *J. Am. Chem. Soc.* **1986**, *108*, 2301.

(45) Randall, L. H.; Cherkas, A. A.; Carty, A. J. *Organometallics* **1989**, *8*, 568.

(46) (a) Johnson, B. F. G.; Benfield, R. E. In *Transition Metal Clusters*; Johnson, B. F. G., Ed.; John Wiley and Sons: Chichester, U.K., 1980; Chapter 7. (b) Band, A. E.; Muetterties, E. L. *Chem. Rev.* **1978**, *78*, 639. (c) Evans, J. *Adv. Organomet. Chem.* **1977**, *16*, 319. (d) Cotton, F. A. In *Dynamic Nuclear Magnetic Resonance Spectroscopy*; Jackman, L. M., Cotton, F. A., Eds.; Academic Press: New York, 1975.

(47) Colbran, S. B.; Johnson, B. F. G.; Lahoz, F. J.; Lewis, J.; Raithby, P. R. *J. Chem. Soc., Dalton Trans.* **1988**, 1199.

$H)_2Ru_4(CO)_{12}(\mu_3\text{-PPh})$, that in **2a** can be frozen out at 196 K. At intermediate temperatures, the wing tip carbonyl ligands begin to interconvert by a similar mechanism. Shortly after the onset of wing tip carbonyl exchange, three of the four carbonyl ligands bound to Ru(3) broaden in a 3-fold exchange process, leaving a single unique ligand static which only participates in exchange at higher temperatures.

Although qualitatively similar exchange processes occur in $H_2Ru_4(CO)_{12}(\mu_3\text{-PPh})$ and **2a**, there are several notable differences: (i) trigonal rotation at Ru(3) is much more facile in **2a** presumably due to the absence of hydride ligands, (ii) at room temperature and above we observe the onset of facile intermetallic CO migration in **2a**, and (iii) all carbonyl motion can be frozen out at 196 K in **2a**. While the carbonyl fluxionality in **2b** was not investigated in detail due to the compound's low solubility, the room-temperature $^{13}C\{^1H\}$ NMR spectrum was also indicative of exchange.

Conclusions

The clusters $(\mu\text{-H})Ru_3(CO)_{10}(\mu\text{-PPh}_2)$ (**1a**) and $(\mu\text{-H})Os_3(CO)_{10}(\mu\text{-PPh}_2)$ (**1b**) have proven to be suitable precursors for the preparation of the butterfly clusters *nido*-$M_4(CO)_{13}(\mu_3\text{-PPh})$ (M = Ru, Os). The synthesis proceeds via a reductive elimination of benzene/condensation pathway. In the case of the lighter congener, the elimination reaction appears to be induced by the favorable interaction of a P–C(ipso) bond with the unsaturated ruthenium center, contrasting the formation of **2b**, which occurs via the metalated cluster $(\mu\text{-H})_2Os_3(CO)_9\{\mu\text{-P(Ph)}C_6H_4\}$ (**6**) followed by reductive elimination of benzene. Crystals of **2a** and **2b** are isomorphous, providing a unique opportunity for a direct comparison of the structural features of these two homologues. An alternative synthetic procedure for the preparation of $Ru_4(CO)_{13}(\mu_3\text{-PPh})$ consists of the addition of an appropriate dichlorophosphine to the dianion $[Ru_4(CO)_{13}]^{2-}$. Using this procedure we can tailor both the steric and electronic requirements of the phosphinidene stabilizing fragment.

Acknowledgment. We are grateful to the Natural Sciences and Engineering Research Council of Canada for financial support of this work in the form of operating and equipment grants (to A.J.C.) and scholarships (to A.A.C., J.F.C., and S.A.M.).

Supplementary Material Available: For **2a** and **2b**, structural analyses, anisotropic displacement coefficients (Tables S1 and S5), remaining bond lengths and angles (Tables S2 and S6), hydrogen atom coordinates (Tables S3 and S7), and complete crystallographic data (Table S9) (9 pages). Ordering information is given on any current masthead page. Structure factors (Tables S4 and S8, 35 pages) are available from the authors upon request.